Properties of Ternary Sn-Ag-Bi Solder Alloys: Part II—Wettability and Mechanical Properties Analyses

P.T. VIANCO and J.A. REJENT

Center for Solder Science and Technology, Sandia National Laboratories, Albuquerque, NM

Bismuth additions of 1% to 10% were made to the 96.5Sn-3.5Ag (wt.%) alloy in a study to develop a Sn-Ag-Bi ternary composition. Thermal properties and microstructural analyses of selected alloy compositions were reported in Part I. Wettability and mechanical properties are described in this paper. Contact angle measurements demonstrated that Bi additions improved wetting/spreading performance on Cu; a minimum contact angle of $31 \pm 4°$ was observed with 4.83 wt.% Bi addition. Increasing the Bi content of the ternary alloy raised the Cu/solder/Cu solder joint shear strength to 81 MPa as determined by the ring-and-plug tests. TEM analysis of the 91.84Sn-3.33Ag-4.83Bi composition presented in Part I indicated that the strength improvement was attributed to solid-solution and precipitation strengthening effects by the Bi addition residing in the Sn-rich phase. Microhardness measurements of the Sn-Ag-Bi alloy, as a function of Bi content, reached maximum values of 30 (Knoop, 50 g) and 110 (Knoop, 5 g) for Bi contents greater than approximately 4–5 wt.%.

Key words: Sn-Ag-Bi alloys, solder, solid-solution strengthening, microhardness

INTRODUCTION

The wettability properties are critical for developing soldering processes. It is also important to correlate the microstructure of the alloy with its mechanical properties (tensile strength, fatigue resistance, and creep strength) in order to optimize service performance of the interconnect. The microstructural features of the Sn-Ag-Bi alloys, together with their thermal properties, were described in Part I of this report. The present study reports on the mechanical properties as well as the wettability performance of Sn-Ag-Bi ternary alloys.

The Sn-Ag-Bi alloys were fabricated with Bi additions in the range of approximately 1 wt.% to 10 wt.%. The Bi additions were made to keep the ratio of Ag to Sn (in wt.%) the same as that of the eutectic composition 3.627 in order to (1) maximize the melting point depression effects by the Bi additions and (2) develop the largest extent of Sn-rich matrix phase to maximize the amount of Bi in the alloys. Solder joint shear strength was determined from the ring-and-plug shear tests. Microhardness tests were also performed. Wetting and spreading activity by the molten alloy was measured on Cu test pieces using the meniscometer/wetting balance technique.[1]

(Received February 16, 1999; accepted July 22, 1999)

EXPERIMENTAL PROCEDURES

Solderability Measurements

The wetting and spreading behavior (or solderability) of the alloys developed in this study was evaluated using the meniscometer/wetting balance technique.[1] The quantitative metric is the contact angle, θ_c, formed on the surface of a Cu coupon that is immersed edge-on into a bath of molten solder (Fig. 1). The equilibrium contact angle is determined by the interfacial tensions, γ_{SF}, γ_{SL}, and γ_{LF} through Young's equation:

$$\gamma_{SF} - \gamma_{SL} = \gamma_{LF} \cos \theta_c \quad (1)$$

The value of θ_c is computed from two properties of the wetting solder, the height of meniscus rise, H, experienced by the molten solder on the sides of the coupon and the weight of that meniscus, W. The meniscus rise (H) is determined by the meniscometer apparatus that detects the distance of travel by the climbing solder via a high power microscope. The meniscus weight (W) is determined by the wetting balance apparatus. The output of the wetting balance is a

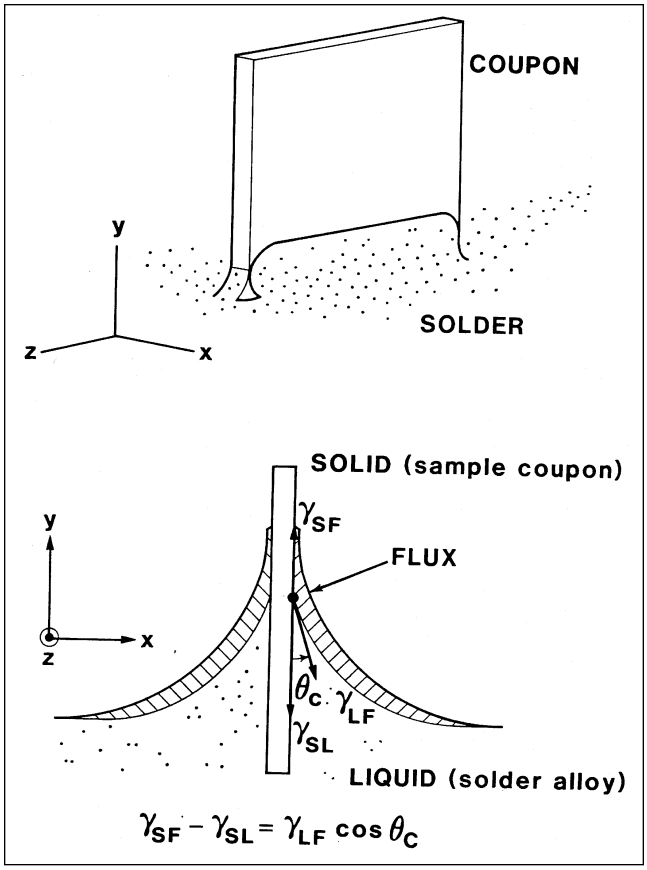

Fig. 1. Sample geometry for the wetting/spreading tests performed on the molten alloys.

trace of the meniscus weight as a function of time (Fig. 2). The maximum meniscus weight is used to calculate θ_c by the following expression:

$$\theta_c = \sin^{-1} \{[4W^2 - (\rho g P H^2)^2] / [4W^2 + (\rho g P H^2)^2]\} \quad (2)$$

where ρ is the solder density, P is the sample perimeter (i.e., twice the coupon width added to twice the coupon thickness), and g is the acceleration due to gravity. In addition to a computation of the contact angle, a similar expression was derived for calculating the value of the solder-flux interfacial tension, γ_{LF}:

$$\gamma_{LF} = (\rho g/4) \{[4W^2 / (\rho g P H)^2] + H^2\} \quad (3)$$

where each of the symbols has the same meaning as listed above. This parameter is particularly sensitive to the solder composition (and the flux) and is an important factor in the wetting/spreading activity of molten metals and alloys.[2] Also provided in the analysis was the wetting rate as well as the wetting time, t_W, both of which are illustrated in Fig. 2.

The test coupons were oxygen-free, high conductivity (OFHC) Cu coupons measuring 25.4 × 25.4 × 0.254 mm. Once cut from the stock material, each coupon was solvent degreased and then immersed in a one-to-one solution of HCl and water for 1 min. The specimens were suitably rinsed, dried, and subsequently coated with a rosin-based, mildly activated (RMA) flux that had been diluted one-to-one with isopropyl

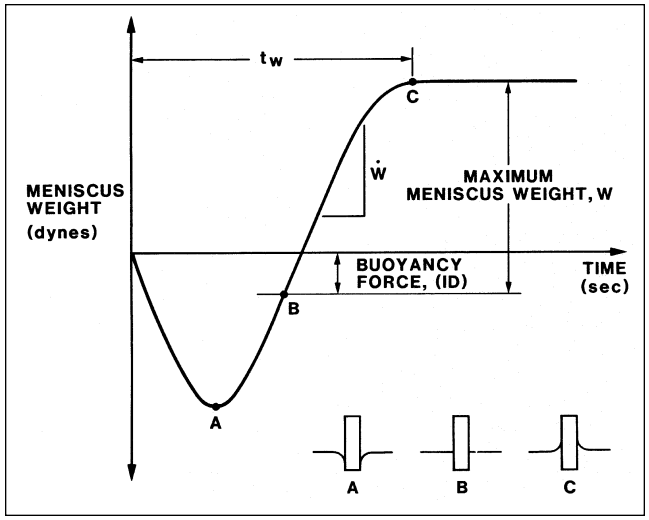

Fig. 2. Wetting balance output plot of meniscus weight versus time.

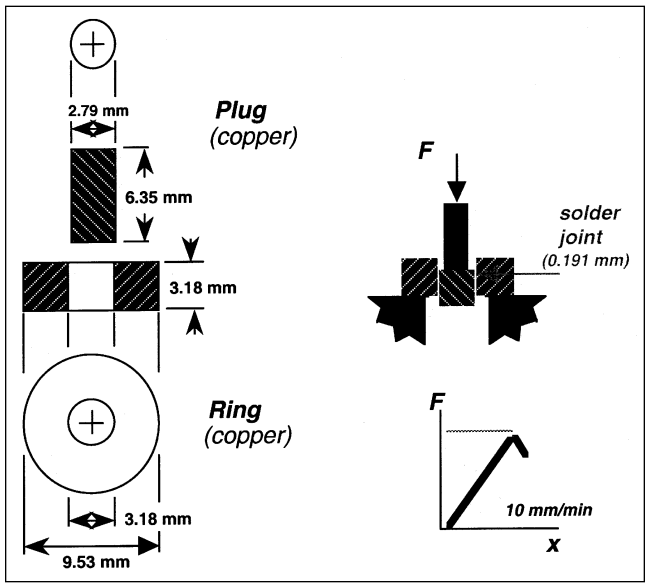

Fig. 3. Specimen dimensions and assembly/test configurations for ring-and-plug, joint shear strength test.

alcohol. In each case, the flux coating was allowed to dry for 10 min prior to testing. Five (5) samples were evaluated for meniscus height, H, and five samples (5) for the meniscus weight, W. Error terms for θ_c and γ_{LF} were computed from the above equations, using maximum and minimum values of H and W, as determined by one standard deviation about the mean of the respective five measurements, that in combination resulted in maximum and minimum values of the θ_c and γ_{LF} parameters. All alloy compositions were evaluated at a temperature of 245°C.

Mechanical Testing

Ring-and-Plug Shear Tests

The mechanical properties of the Sn-Ag-Bi alloys was benchmarked by measuring the shear strength of Cu/Cu joints made with the candidate material. The ring-and-plug test was used; the test specimen geom-

etry is shown in Fig. 3. The specimen consisted of a Cu ring and a Cu plug (solid cylinder), both machined from OFHC Cu stock. The inner (hole) diameter of the ring and the diameter of the plug provided a solder joint gap of 0.195 mm. Both the ring and plug pieces were degreased in an organic solvent, rinsed, and etched by immersing in a 1:1 solution of HCl and H_2O for 1 min. The specimens were then rinsed again and dried. The inner surface of the ring and outer surface of the plug were coated with the same diluted RMA flux solution as was used for the solderability tests described above.

Assembly of the test sample proceeded immediately following application of the flux. The ring was placed into a stainless steel fixture. Three Cu wires of 0.178 mm diameter were positioned at equal intervals about the ring's hole to assure that the same nominal gap dimension was maintained about the entire circumference of the joint.[3] The wires were made of Cu and cleaned in the same manner as were the ring and plug parts to assure that the wires were wet by the solder. Next, the plug was put into place followed by a donut preform of the Sn-Ag-Bi alloy, which was slipped down about the plug so as to rest on the top surface of the ring. The entire assembly was then placed on a hot plate that was set at between 350°C and 400°C. Once the preform had melted, the specimen remained on the hot plate for an additional 15 s to assure capillary flow of the molten solder through the gap. Each specimen was carefully removed from the hot plate and placed on a chill block to expedite cooling. The cooling rate of the joints was not recorded, although its consistency between samples was assured by carefully repeating the detailed assembly procedure.

The final geometry was provided by the following procedure. The portion of the plug that extended beyond the top and bottom surfaces of the ring was cut off with a slow-speed diamond saw. Then, both sides of the specimen were ground to remove any remaining vestige of the plug that extended beyond the ring to guarantee that the two surfaces were parallel. Parallelism was verified. It was also confirmed that the cutting and polishing procedures did not damage the joints.

The mechanical strength test was performed by placing the specimen into a stainless steel holder. The test machine cross head applied a force to the plug through a punch made of Inconel™718 (INCO Alloys, Inter., Huntington, VA). The test was performed under a constant displacement rate of 10 mm/min (0.4 in./min). For each solder alloy, a total of five ring-and-plug samples was fabricated. Mechanical tests were performed on four of the five specimens; the data was represented as the mean and + one standard deviation of the maximum load values measured from the plots of the four tests. The fifth sample was cross sectioned for metallographic observation of the solder joint microstructure. The maximum shear stress was calculated, based upon the centerline surface of the gap and the maximum load.

Microhardness Tests

Microhardness tests were performed with a Knoop indentor using 5 or 50 g loads. The hold time was 15 s. Five tests were performed per alloy; the data were represented as the mean of those five measurements and + one standard deviation.

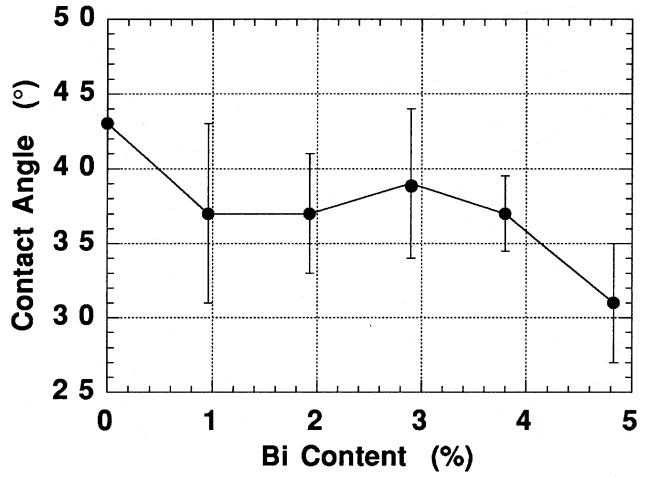

a

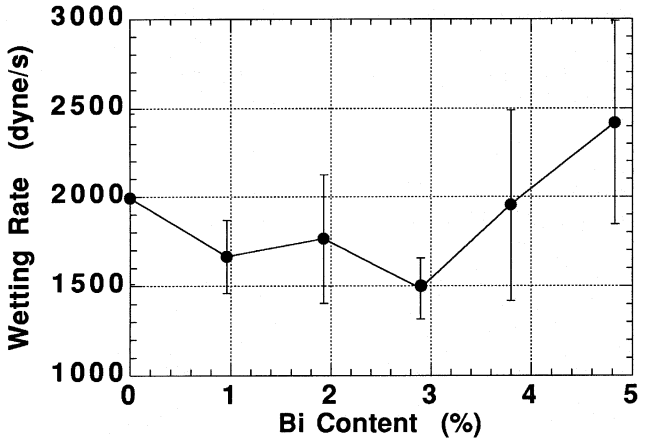

b

Fig. 4. (a) The contact angle and (b) the wetting rate of the Sn-Ag-Bi alloys as a function of Bi content. The solder working (test) temperature was 245°C for all Sn-Ag-Bi compositions and 248°C for the 96.5Sn-3.5Ag alloy. The same RMA flux was used in all experiments.

RESULTS

Solderability Measurements

The contact angle measurements were performed on the following Sn-Ag-Bi ternary compositions:

95.57Sn-3.47Ag-0.96Bi
94.63Sn-3.44Ag-1.93Bi
93.70Sn-3.40Ag-2.90Bi
92.76Sn-3.37Ag-3.87Bi
91.84Sn-3.33Ag-4.83Bi

It was recognized that the alloy onset temperatures varied with Bi content, from 218°C (0.96Bi) to 212°C (4.83Bi). It was inferred from a prior solderability

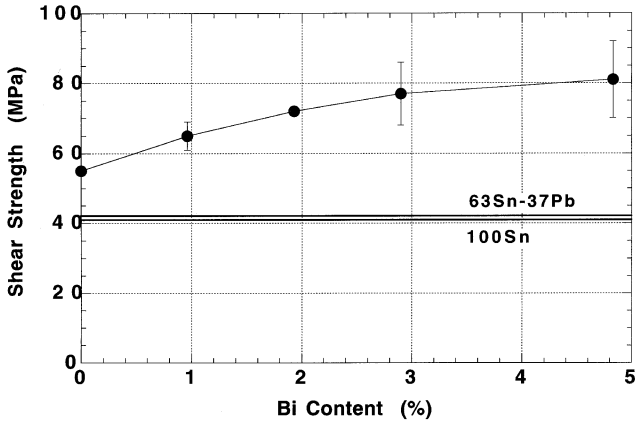

Fig. 5. Ring-and-plug shear stress data as a function of Bi content. Also included are stress values from similarly tested 100Sn and 63Sn-37Pb alloy. The testing rate in all cases was 10 mm/min.

study of Sn-Pb solders and a Fe-Ni-Co alloy base material that differences between the onset temperatures of the respective Sn-Ag-Bi alloys and the solder pot temperature of 245°C were not sufficiently large so as to impact the relative solderability performances.[4] Thus, the contact angle data should reflect largely compositional effects.

Graphs of (a) the contact angle and (b) the wetting rate as functions of Bi content are shown in Fig. 4. Also included in the graphs is the datum for the 96.5Sn-3.5Ag (0%Bi) solder that was tested at 248°C as part of a previous investigation.[5] The data points were connected for clarity, only; no functional trend is implied. The mean contact angle data in Fig. 4a indicated that Bi additions to the Sn-Ag binary alloy of up to 3.87% resulted in a decrease in the mean contact angle values. However, this apparent improvement in solderability was obscured by the scatter experienced in the measurements. A more substantial decease in contact angle was realized when the Bi addition was raised to 4.83%, giving a contact angle value of 31 ± 4°. It was further determined that the improvement in solderability associated with the 4.83Bi content was due in large part to a decrease in the solder-flux interfacial tension, γ_{LF}, as calculated using Eq. 3. A decrease in γ_{LF} was expected with the Bi additions, given the low surface tension of molten Bi (375 dyne/cm at 350°C) relative to values for Sn (550 dyne/cm at 232°C) and Ag (895 dyne/cm at 1000°C).[6] The γ_{LF} declined from a value of 490 ± 80 dyne/cm for the 96.5Sn-3.5Ag eutectic to 418 ± 20 dyne/cm for the 4.83Bi addition.

A plot of the wetting speed as a function of Bi content in the Sn-Ag-Bi alloys is shown in Fig. 4b. A slight decrease in the mean wetting rate appeared discernible for Bi contents in the range of $0 < Bi < 2.90$. The values then increased sharply for Bi additions of 3.87% and 4.83%. Unfortunately, the unusually large data scatter exhibited by these measurements precluded a strong statistical significance to the observed trends. The precise mechanism by which the Bi content impacted the wetting and spreading kinetics remains unclear.

The wetting and spreading properties of the 91.84Sn-3.33Ag-4.83Bi alloy were also tested at 230°C and 260°C. Contact angles of 33 ± 4° and 31 ± 3°, respectively, were measured. These values were not significantly different from the 31 ± 4° value measured at 245°C. This trend has been observed in a previous study that indicated a relative insensitive of the contact angle to the solder temperature.[4] The solder-flux interfacial tension (γ_{LF}) was not observed to be strongly affected by a similar, limited range of test temperatures. On the other hand, the wetting speed increased sharply at the higher temperature of 260°C and decreased when the solder temperature was dropped to 230°C, relative to the behavior at 245°C. These trends affirmed observations from previous studies that the test temperature had a significant impact on the speed of the wetting/spreading process.[4]

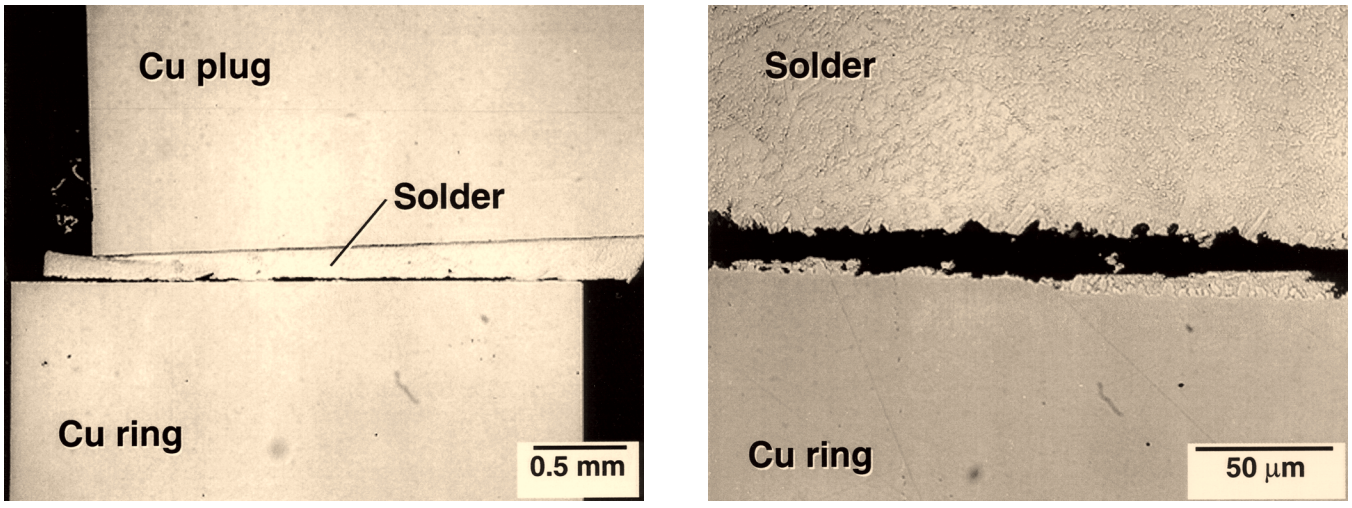

a b

Fig. 6. Optical micrographs of the ring-and-plug test sample fabricated with the 95.57Sn-3.47Ag-0.96Bi solder: (a) low magnification and (b) high magnification.

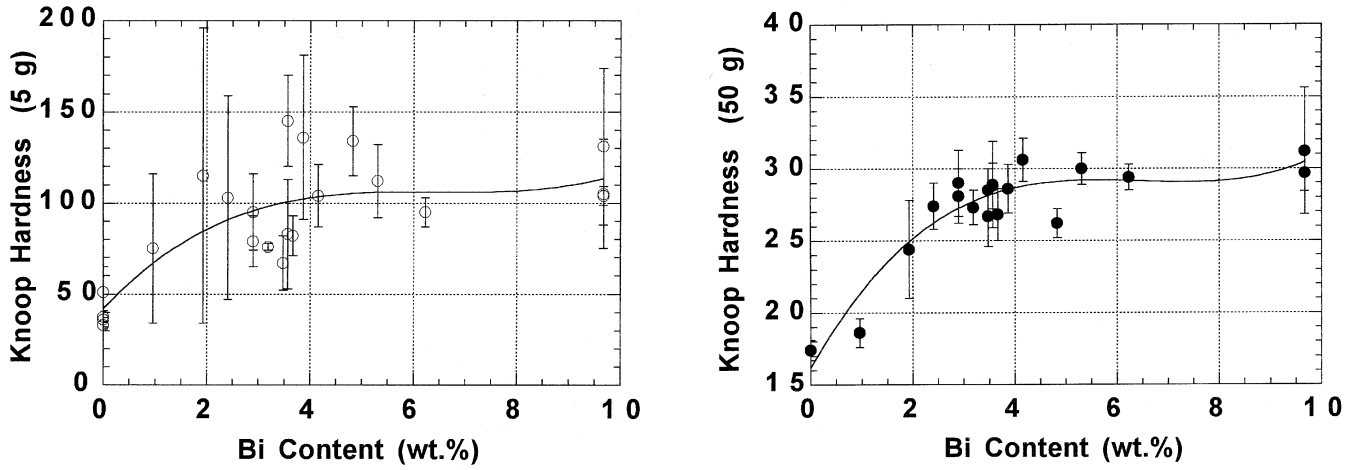

a b

Fig. 7. Microhardness data for Sn-Ag-Bi alloy compositions as a function of Bi content using the Knoop indentor and probe loads of (a) 5 g and (b) 50 g. The data were presented as the mean value and an error bar indicating ± one standard deviation. The lines represent the third-order polynomial fit by the least squares method.

Mechanical Testing— Ring-and-Plug Shear Test

The following four Sn-Ag-Bi ternary alloys were evaluated by the ring-and-plug test procedure:

95.57Sn-3.47Ag-0.96Bi
94.63Sn-3.44Ag-1.93Bi
93.70Sn-3.37Ag-2.90Bi
91.84Sn-3.33Ag-4.83Bi

The shear strength data as a function of Bi content are shown in Fig. 5. Also included in Fig. 5 are test results for 63Sn-37Pb alloy and 100Sn. As the Bi content of the ternary alloy increased, so did the mean shear strength of the ring-and-plug specimens. In the case of the 91.84Sn-3.33Ag-4.83Bi composition, the shear strength was nearly twice the value from that of similar measurements on the 63Sn-37Pb and 100Sn materials. The high strength of the 91.84Sn-3.33Ag-4.83Bi alloy was attributed to two phenomena—a solid-solution strengthening effect by the Bi dissolved in the Sn-rich phase and a precipitation strengthening effect by the larger Bi particles. In addition, the Bi addition caused a more homogenous dispersion of Ag_3Sn phase particles in the Sn-rich matrix which may have further enhanced the alloy strength.

The data trend in Fig. 5 suggests that the strength may level off at Bi level greater than approximately 5 wt.%. In fact, Bi additions at 4–5 wt.% represent a saturation point for Bi to remain in solution within the Sn-rich matrix (Fig. 3, Part I). Greater Bi contents would, therefore, not be expected to contribute additional strength through the solid solution mechanism. However, some added strength may be realized from Bi contents exceeding the 5 wt.% level by an enhanced precipitation strengthening mechanism.

Metallographic cross sections were made of selected ring-and-plug samples representing the Sn-Ag-Bi compositions. Shown in Fig. 6 are (a) low and (b) high magnification micrographs of the failure mode

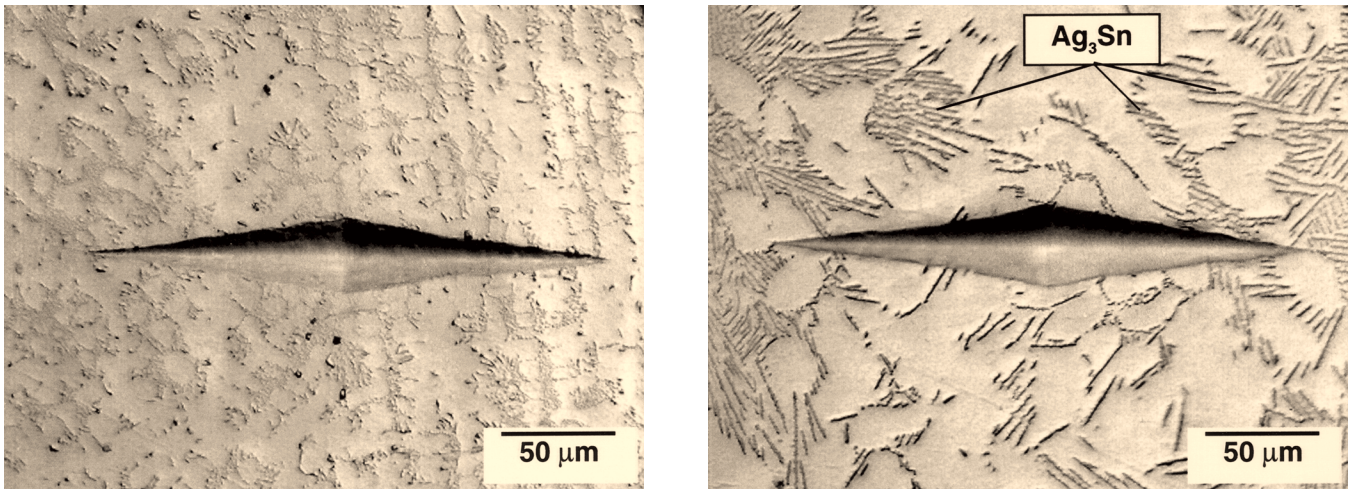

a b

Fig. 8. Optical micrographs of the 100 g Knoop indentations placed into the alloys (a) Sn-Ag-2.9Bi and (b) Sn-Ag-3.57Bi, comparing the indentation size scale to the two different scales of microstructure.

for the sample made with the 95.57Sn-3.47Ag-0.96Bi alloy. The observed fracture morphology of this alloy was representative of the other Sn-Ag-Bi ternary solders. The fracture path occurred near to the solder-substrate interface, but remained in the solder. The crack did not propagate within the intermetallic compound layer.

Microhardness

The microhardness study was performed on all of the Sn-Ag-Bi alloys listed in section 2.1. The tests were performed with the Knoop indentor, using loads of 5 g and 50 g. The hardness values as a function of Bi content are shown in Fig. 7. The hardness values as a function of Bi content were fit to a third order polynomial by the least-squares fit methodology; those traces are also shown in each of the plots. Similar trends were recorded for both the 5g and 50 g load tests. The mean hardness values exhibited an initial increase for 0% Bi to 4-5% Bi levels. Bismuth additions of 5% to 10% did not appear to cause any further change to the hardness. The same generalized behavior was observed with the ring-and-plug shear stress data (Fig. 5).

Several observations can be made from the data in Fig. 7. First, the scatter in the data was generally less with the 50 g load. Second, a relative comparison of the scatter values suggested a similar scatter pattern characterized measurements from both 5 g and 50 g loads. For example, the Sn-Ag-Bi compositions with 1.93Bi and 9.67Bi had relatively large data scatter at both the 5 and 50g applied loads while the ternary alloy having 6.23Bi had a more limited data scatter under either load. These observations suggest that the trends in the hardness scatter were intrinsic to a particular solder composition (Bi content) and were not solely an artifact of the applied load or test techniques.

The data scatter did not appear to be sensitive to the size scale of the distribution "network" of Ag_3Sn particles in the Sn matrix. The Ag_3Sn network coarsened in the Sn-Ag-Bi alloys as Ag_3Sn particles dispersed with increasing Bi additions. This point is shown in the two micrographs in Fig. 8 which show 100 g Knoop hardness impressions (which have approximately the same size as the 50 g load marks) placed into samples of (a) the Sn-Ag-2.9Bi alloy and (b) the Sn-Ag-3.57Bi alloy. In the former case, the indentation dimensions were considerably larger than the size scale of the Ag_3Sn features. The coarser microstructure of the ternary alloy with 3.57 wt.%. Bi had a size scale that was comparable to that of the hardness indentation. Yet, the scatter in the hardness data from the two alloy microstructures was very similar. The apparent insensitivity of the hardness behavior to the Ag_3Sn network size suggests that this microstructural feature was inconsequential to the hardness property. Rather, the hardness behavior was determined primarily by the properties of the Sn-matrix.

SUMMARY

(1) Bismuth additions of approximately 1% to 10% were made to the baseline 96.5Sn-3.5Ag (wt.%) alloy to fabricate Sn-Ag-Bi ternary compositions. The ratio of Ag to Sn was constant for all cases. Test data on the thermal and microstructural properties of selected Sn-Ag-Bi alloys were reported in Part I.

(2) Solderability experiments (contact angle metric) demonstrated that Bi additions improved wetting and spreading performance. At the 4.83 wt.% Bi concentration, a minimum contact angle of $31 \pm 4°$ was observed. The contact angle showed minimal sensitivity to solder temperatures of 230°C to 260°C.

(3) The Cu/solder/Cu shear strength, as determined by the ring-and-plug test, increased with Bi content of the ternary alloy. TEM analysis in Part I confirmed that the strength improvement was attributed to solid-solution and precipitation strengthening effects by Bi in the Sn-rich phase.

(4) Microhardness measurements on the Sn-Ag-Bi alloy increased with greater Bi content, and appeared to reach maximum values of 30 (Knoop, 50 g) and 110 (Knoop, 5 g) for Bi exceeding approximately 4–5 wt.%.

ACKNOWLEDGMENTS

The authors wish to thank M. Dvorack for his critical review of the manuscript and A. Kilgo for metallographic sample preparation. this work was supported by the U.S. Dept. of Energy under contract DE-AC04-94AL85000. Sandia is a multiprogram laboratory operated by Sandia Corp., a Lockheed Martin Co., for the U.S. Dept. of Energy.

REFERENCES

1. P. Vianco, *The Metal Science of Joining*, ed. M. Cieslak et al. (Warrendale, PA: TMS, 1992), pp. 265–284.
2. P. Vianco and A. Claghorn, *Soldering and Surf. Mount Tech.* 12 (1996).
3. K. Stone, R. Duckett, S. Muckett, and M. Warwick, *Brazing and Soldering* volume, 20 (1983).
4. P. Vianco, F. Hosking, and J. Rejent, *Welding Journal Res. Suppl.* 69, 232 (1990).
5. A. Jackson, I. Artaki, and P. Vianco, *Proc. 7th Inter. SAMPE Conference* (Covina, CA: SAMPE, 1994), pp. 381–393.
6. L. Murr, *Interfacial Phenomena in Metals and Alloys* (Reading, MA: Addison-Wesley, 1975), pp. 101–106.